TELKOMNIKA Indonesian Journal of Electrical Engineering
Vol.12, No.4, April 2014, pp. 2743 ~ 2752
DOI: http://dx.doi.org/10.11591/telkomnika.v12i4.4368

An Adaptive Detection Method of Multiple Faces

Wei Li
China West Normal University, No. 1 Shida Road, Computer School, Nanchong, China
*Corresponding author, e-mail: nos036@163.com

Abstract

The appearance of multiple faces is influenced by abnormal exposure, interfering backgrounds or fake objects greatly in the color face image. A multiple-face detection method based on the adaptive dual skin model and improved fuzzy C-mean clustering was presented in this study. First an adaptive skin-color model and an adaptive skin-probability model were built to acquire the skin likelihood for clustering, the adaptive initial clustering centers, and the adaptive clustering weights. Then the skin-likelihood image was segmented dynamically by improved fuzzy C-mean clustering. Finally the multiple-face targets were distinguished and extracted by jointly using the effective areas, circumferences and circularities of connected targets. Experiment showed that the algorithm had good results and high speed, accuracy, and adaptability of face detection.

Keywords*: skin model, face detection, fuzzy clustering, connected component labelling*

1. Introduction

The face recognition is an active subject in the fields of computer vision and pattern recognition, which has a wide range of potential applications. The face recognition is an active subject in the fields of computer vision and pattern recognition, which has a wide range of potential applications [1]. On the matter of single-face detection under the conditions of simple background and uniform exposure, the face detection method based on skin color model can achieve good results because of the compactness of skin color clustering distribution [2-5]. For fast multiple-face detection under complex backgrounds, the stability, accuracy, adaptability, anti-interference, and applicable conditions of the existed detection method still had some limitations. Ruiz-del-Solar and Quinteros [6] made a study of preprocessing approaches, Zhang et al. [2] realized the single-face detection in complex background, Shih et al. [3] realized the multiple-face detection, but the method was greatly affected by illumination, imaging device, and the interfering backgrounds or fake objects. Wang and Li [4] combined the Gaussian mixture model and template matching, but the parameter estimation of model and the template matching cost too much time of calculation. Hsu et al. [5] used the ellipse skin model to segment the skin regions, but the method need lighting compensation, and to census lots of skin samples for calculating the fixed model parameters that maybe not suitable for the certain input image. Its anti-interference and the scope of application are limited.

Some people [7-10] provided the method based on AdaBoost or neural network, but their methods required training samples, the accuracy of detection was greatly affected by training samples and test images, and the training or learning was time-consuming. Facing these problems, for face images with abnormal exposure and interfering backgrounds, this study proposed a fast adaptive multiple-face detection method. To ensure the fast speed, adaptability, and higher detection accuracy, this method need not preprocess, train classifiers, and adopt fixed statistical parameters that depend on sample sets. It is realized based on a self-established dual skin model, which contains a self-defined YIC skin model and a self-defined YIQ skin-probability model. Based on the YIC skin model, it acquired the skin likelihood and adaptive initial clustering centers. Based on the YIQ skin-probability model, it acquired the adaptive clustering weights. Then the fuzzy C-means (FCM) clustering was improved to segment the skin regions fast and dynamically. After skin segmentation, the areas, circumferences, and circularities of the connected targets were used jointly for finishing the multiple-face detection finally.

Received Aug 19, 2013; Revised Oct 23, 2013; Accepted Nov 16, 2013

2. The Algorithm Flow

The multiple-face detection flow is depicted in Figure 1, as the following stages:

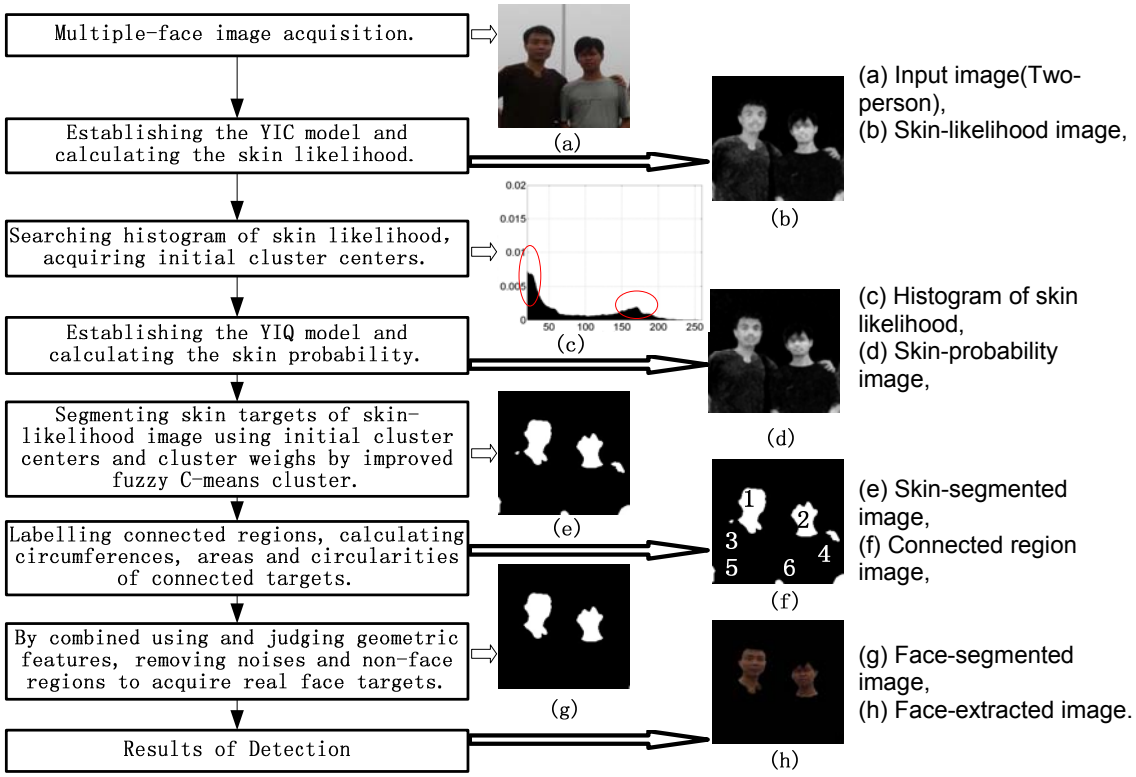

Figure 1. The Flow of Detection Algorithm and Involved Image in Every Stage

Stage 1: Multiple-face image acquisition.
Stage 2: Establish the adaptive YIC skin-color model for multiple-face input image, based on which calculate the skin-color likelihood and acquire the skin-likelihood image.
Stage 3: Based on the skin-likelihood image, automatically search its smoothed gray histogram, and acquire the initial fuzzy clustering centers.
Stage 4: Establish the adaptive YIQ skin-probability model for multiple-face input image, based on which calculate the skin probability and acquire the skin-probability image.
Stage 5: Regard the skin probability as the adaptive fuzzy clustering weights. Using the adaptive initial clustering centers and fuzzy clustering weights, segment the skin targets of the skin-likelihood image fast and dynamically by improved FCM clustering, and acquire the skin-segmented image.
Stage 6: Label the connected targets (the face candidates) in the skin-segmented image. Calculate the geometric features (the effective areas, circumferences, and circularities) of the connected targets.
Stage 7: By jointly using and limiting the geometric features, remove the noises and the non-face regions to distinguish and acquire the real face regions.
Stage 8: Output the extracted face targets.

3. Skin Region Segmentation

3.1. The Dual Skin Model for Multiple-face Input Image

Variety of color spaces applied to problems of skin-color detection [11, 12] or segmentation method [13], such as normalized RGB, YCbCr, YIQ, HSV, and TSL. The YCbCr color space used widely in kinds of existing skin-color models, such as Gaussian model [3, 4,

12], and ellipse model [2, 5]. To segment the multiple-face targets effectively under the conditions of complex backgrounds, fake objects, or abnormal exposure, a reliable skin model is needed. Considering not only the model can reflect the characteristic of distribution of skin color, but also it has good stability, anti-interference and adaptability, this study planed to establish an adaptive dual skin-color model. The established model fused features of multiple components and combined the improved fuzzy clustering, which increased the speed and accuracy of clustering to realize the skin segmentation. Concerning the dual skin-color model, the first model was used to calculate the skin likelihood and acquire the skin-likelihood gray image for clustering, analyzing, and obtaining the initial clustering centers. The second model was used to acquire the necessary information such as the clustering weights that can enhance the effect and ability of clustering. By analysis, I component in YIQ color space covered the range of skin color, and represents the tone range from bisque to blue-green. The Cb, Cg, and Cr are three chrominance components independent from Y luminance component. If the influence of luminance (Y) could be depress, besides I component and differences of three chrominance components could be combined in an adaptive skin model, it is very beneficial for improving anti-interference and adaptability of segmentation. Based on this idea, an adaptive YIC model fused multiple components of Y, I, Cb, Cg, and Cr was built (Equation (2)).

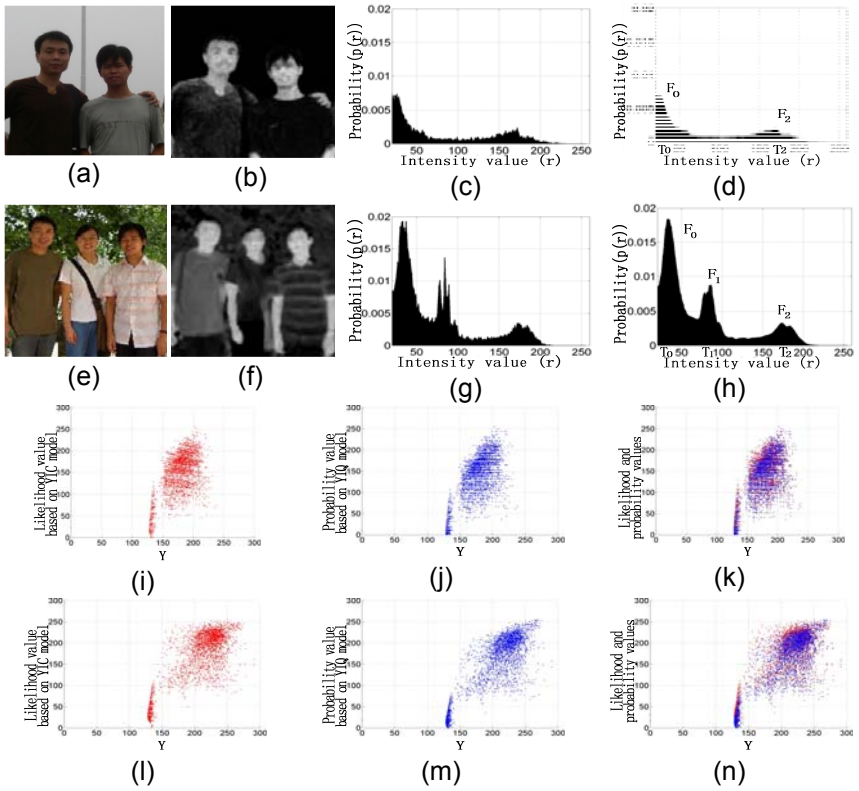

(a) Original image 1, (b) likelihood image 1, (c) histogram of (b)(burrs), (d) smoothed histogram of (c)(two peaks), (e) Original image 2, (f) likelihood image 2, (g) histogram of (f)(burrs), (h) smoothed histogram of (g)(three peaks), (i) skin-likelihood distribution of (a), (j) skin-probability distribution of (a), (k) Comparison of distribution of (i) and (j), (l) skin-likelihood distribution of (e), (m) skin-probability distribution of (e), (n) Comparison of distribution of (l) and (m).

Figure 2. The Analysis of the Adaptive Skin Likelihood and Skin Probability

As Figure 2 showed, the Figure 2(a) is a multiple-face color image with underexposure, the Figure 2(e) is a multi-face color image with complicated backgrounds and uneven exposure. Based on the built YIC model, the acquired normalized adaptive likelihood gray image, the likelihood gray histogram, and the smoothed histogram are showed in Figure 2(b)-(d) and Figure 2(f)-(h), the skin-likelihood distribution image are shown in Figure 2(i) and 2(l). From the distribution, the normalized skin-likelihood values based on the YIC model can reflect the compactness and stability of real skin distribution well. Moreover the smoothed histogram approximately showed the double-peak curve or three-peak curve. This indicated that most of the pixel values of normalized likelihood image concentrated on two to three main gray levels,

as showed in Figure 2(d) and (h). Note that there are two peaks (F_0 and F_2) in Figure 2(d), and there are three peaks (F_0, F_1, and F_2) in Figure 2(h). The sharp-pointed maximum peak F_0, which represented the number of pixels in background regions, is near to 0 gray level or in the range of low gray levels. The possible sharp-pointed second maximum peak F_1, which represented the number of pixels in non-skin or fake-skin regions, is located in the range of low gray levels. The flat peak F_2, which represented the number of pixels in skin regions, is located in the range of middle or high gray levels.

Considering that the FCM clustering algorithm is sensitive to the initial clustering centers and the speed and effect of the clustering maybe unstable because of the difference of initial clustering centers, this study improved the FCM clustering to realize the dynamic skin region segmentation. The main idea of improved FCM algorithm is as follows: based on the traditional FCM algorithm, the gray levels of peaks in skin-likelihood histogram was regarded as the initial fuzzy clustering centers to decrease the invalid computation of clustering, and to greatly improve the speed, effect and adaptability of clustering. In addition, another adaptive YIQ skin-probability model (Equation (5)) was established. The acquired skin probability values based on the YIQ model reflected the degree of skin probability. The skin probability was regarded as the adaptive weights of fuzzy clustering to update the clustering centers, and to achieve the purposes of improving the speed of clustering and acquiring the better segmentation.

The built adaptive YIQ skin-probability model combined the differences between I, Q, and Y components, and the difference between I component and its expectation ($\bar{I}$), as shown in Equation (5). The distribution of the skin probability based on the YIQ model is approximately close to the distribution of the normalized skin likelihood based on the YIC model, as shown in Figure 2. To the skin targets in Figure 2(a) and (e), the Figure 2(i) and (l) show the skin-likelihood distribution based on YIC model, the Figure 2(j) and (m) show the skin-probability distribution based on YIQ model, the Figure 2(k) and (n) show the fitness of the two distributions.

As mentioned before, for the subsequent clustering segmentation, the initial clustering centers was acquired by searching the skin-likelihood histogram of the YIC model, the skin probability of the YIQ model was regarded as the clustering weights in this study. This method actually combined the two kinds of adaptive models, which had the good ability of description to the clustering distribution of skin targets. As the distributional pattern and gray levels range of the skin likelihood and the skin probability were close to each other approximately, the initial clustering centers (came from skin likelihood) and the probabilistic weights (skin probability) was used for fuzzy clustering not only avoided the divergence and uncontrollability of clustering, but also decreased the massive calculation for invalid clustering. By this way, the searching for the skin targets by the adaptive clustering quickly and accurately can be realized.

3.2. The Improved Fuzzy C-means Cluster used for Skin Segmentation

Based on the adaptive dual skin model, the skin segmentation can be realized according to the following steps:

Step 1: Acquire the Y, I, Q, Cb, Cr, and Cg components of input image by Equation (1).

$$\begin{bmatrix} Y \\ I \\ Q \\ Cb \\ Cg \\ Cr \end{bmatrix} = \begin{bmatrix} 128 \\ 0 \\ 0 \\ 128 \\ 128 \\ 128 \end{bmatrix} + \begin{bmatrix} 0.114 & 0.578 & 0.299 \\ -0.322 & -0.274 & 0.596 \\ -0.311 & -0.523 & 0.212 \\ 0.500 & -0.3313 & -0.1687 \\ -0.184 & 0.500 & -0.316 \\ -0.0813 & -0.4187 & 0.500 \end{bmatrix} \begin{bmatrix} B \\ G \\ R \end{bmatrix} \quad (1)$$

Step 2: Establish the adaptive YIC skin model using Y, I, Cb, Cr, and Cg components, based on which calculate the adaptive skin likelihood ($P_{i,j}$) by Equation (2).

$$P_{i,j} = \sqrt[3]{\frac{(Cb-Cr)^2 \times I}{Y}} + \sqrt[3]{\frac{(Cg-Cr)^2 \times I}{Y}} + \sqrt[3]{\frac{((Cb+Cg)/2-Cr)^2 \times I}{Y}} \quad (2)$$

Where, i and j are the horizontal and vertical coordinates of every pixel in input image.

Step 3: Acquire the likelihood gray image (T_p) using the skin likelihood ($P_{i,j}$) by Eq. (3), normalize the gray levels to the range of [0 255], and acquire the normalized likelihood gray image (T_p') by Eq. (4), as shown in Figure 2(b), 2(f) and Figure 3(d).

$$P' = P_{i,j} \times 255 \tag{3}$$

$$P''=\begin{cases}0 & \text{else}\\ 255\times(P'-P'_{min})/(P'_{max}-P'_{min}) & \text{if } (P'_{max}-P'_{min})>0\end{cases} \tag{4}$$

Where, i and j are the horizontal and vertical coordinates of every pixel, P' and P'' are the gray values of non-normalized and normalized likelihood image (T_p and T_p').

Step 4: Acquire the one-dimensional histogram of normalized likelihood gray image (T_p'), as shown in Figure 2(c) and 2(g), average the three neighborhoods of gray levels to smooth the histogram burr, and acquire the smoothed histogram, as shown in Figure 2(d) and 2(h). In the range of [50 250], search the positions of gray levels (T_1 and T_2), which the peaks (F_1 and F_2) in histogram were located in. If the T_1 is not found, there are only the two peaks F_0 and F_2, so T_1=0. Regard the T_1 and T_2 as the gray levels of initial FCM clustering centers.

Step 5: Calculate I and Q parameters and their expectations ($\bar{I}$ and $\bar{Q}$) required by YIQ skin-probability model. Using I and Q components and their expectations, acquire the difference (W') between I and its dynamic expectation ($\bar{I}$) (indicating the skin probability, as the adaptive weights of fuzzy clustering). That means, calculate the adaptive clustering weights W' by Equation (5) to acquire the weights gray image T_w, normalize the weights to the range of [0 255] by Eq. (6) to acquire the normalized adaptive clustering weights gray image T_w' (Figure 3(e)) for updating the FCM clustering centers.

$$W' = \left| I - \bar{I} \times (\bar{I}/\bar{Q} + \bar{I}/\bar{Y}) \right| \tag{5}$$

$$W''=\begin{cases}0 & \text{else}\\ 255\times(W'-W'_{min})/(W'_{max}-W'_{min}) & \text{if } (W'_{max}-W'_{min})>0\end{cases} \tag{6}$$

Where, W' and W'' are the non-normalized and normalized adaptive clustering weights. T_w and T_w' are the clustering weights gray images.

Step 6: Segment the normalized likelihood image (T_p') and acquire the binary skin-segmented image T_b by improved FCM clustering.

3.3. The Improved Fuzzy C-means Cluster used for Skin Segmentation

Use normalized adaptive likelihood image (T_p'), initial clustering centers (T_1 and T_2), and adaptive clustering weight (W'') to improve traditional fuzzy C-means cluster. The procedures of improved FCM clustering algorithm are described as follows:

Step 1: The number of samples (n) in the initial sample set ($\{x_i(i=1,2,\ldots,n)\}$) is the total number of pixels in the normalized adaptive likelihood image T_p', that is, n=h×w (h and w are height and width of T_p'). Set the number of clustering centers (c=2) and the weighed exponent (b=3) that can control the fuzzy degree of clustering.

Step 2: Initialize the sample set $\{x_i(i=1,2,\ldots,n)\}$ contained n samples. Initialize the clustering centers ($C_j(j=1,2,\ldots,c)$) and the membership function ($\mu_{ij}(i=1,2,\ldots,n;\ j=1,2,\ldots,c)$), and the μ_{ij} represents the probability of the first i sample (x_i) belongs to the class j.

Step 3: According to the improved membership function (Equation (11)) of FCM, use the current clustering centers (C_j) to calculate the value (μ_{ij}') of membership degree. According to the computational formula of clustering center (Equation (10)), use the new value of membership degree (μ_{ij}') to update the clustering centers (C_j). According to the Equation (10) and (11), make the clustering centers approximate the target position from the initial position by continuous iteration.

For traditional FCM clustering algorithm, the computational formula of membership degree is described by Eq. (9), and the computational formula of clustering centers is described by Equation (10). The Equation (9) and (10) are acquired by limiting the total membership

degree (Equation (7)) of samples to every class in data set and finding the minimum of value function (Equation (8)).

$$\sum_{j=1}^{c}\sum_{i=1}^{n}\mu_{ij}=1 \tag{7}$$

$$J_i=\sum_{j=1}^{c}\sum_{i=1}^{n}(\mu_{ij})^b\left\|x_i-C_j\right\|^2 \tag{8}$$

$$\mu_{ij}=\left(1/\left\|x_i-C_j\right\|^2\right)^b\Big/\sum_{k=1}^{c}\left(1/\left\|x_i-C_k\right\|^2\right)^b \qquad \text{i=1,2,..., n , j=1,2,..., c} \tag{9}$$

$$C_j=\sum_{i=1}^{n}(\mu_{ij})^b x_i\Big/\sum_{i=1}^{n}(\mu_{ij})^b \quad \text{, j=1,2,..., c} \tag{10}$$

Based on traditional FCM, this study introduced the gray value of pixels in normalized clustering weights image T_w' (Figure 3(e)) into computational formula of membership degree. That means the adaptive skin probability was regarded as adaptive clustering weight (W'') to improve the formula of membership degree, as shown in Equation (11).

$$\mu_{ij}'=\left(1/\left\|x_i-C_j\right\|^2\right)^b W_i''\Big/\sum_{k=1}^{c}\left(1/\left\|x_i-C_k\right\|^2\right)^b W_i'' \quad , \qquad \text{i=1,2,..., n , j=1,2,..., c} \tag{11}$$

Step 4: After each of updating the clustering centers in the process of interaction, calculated the value function by Equation (8), and determined whether the change of the current value relative to the last value of value function was less than the threshold value ($K=1\times10^{-9}$). If the change was less than threshold, which represented the algorithm was convergent, so stopped the clustering, or else returned to cyclically execute the Equation (11) and (10), continued the execution and stopped the clustering until the change of value function was less than the threshold value.

The skin-segmented image (T_b) segmented by the improved FCM is shown in Figure 3(f). Comparing the segmented results based on the Gaussian and Ellipse model in Figure 3(b) and (c), the error segmentation was obviously reduced in Figure 3(f). According to the standard targets, the average segmentation accuracy of the improved FCM clustering to the targets reached more than 95%.

4. Multiple Faces Detection

As shown in Figure 3(f), in the skin-segmented image segmented by the improved FCM clustering, there still were some possible noises and non-skin or false-skin non-face targets. To extract the real face targets, this study combined used and limited the geometric features (the effective areas, circumferences, and circularities) of connected targets to remove noises and non-face targets. By the statistics and analysis of the face objects (with backgrounds or fake targets, non-simple face) in the multiple-face set, it is found that, the multiple-face target often was smaller in size than the single-face target, but was larger than the noise. After normalized zooming the multiple-face image to the size of 150×150 pixels, the most of effective areas of multiple-face targets were in the range of 0.5%~90% of the total areas (Equation (12)). If the effective area ratio of a connected target was bigger than 90%, the target maybe a single face. If the effective area ratio (S_K/S) of a connected target was smaller than 0.5%, the target maybe the noise or non-face small region. Vital few targets were the tiny faces, which can be seen as the noise because it did not have enough information to finish subsequent processing, such as the facial features extraction. The most of circumferences (Equation (13)) of the real multiple-face targets were in the range of 10~22500 pixels (The boundary length of the whole normalized zoomed image was 22500 pixels. The most of circumferences of the noise or non-face small regions was smaller than 10 pixels). Thus, this study removed the noises and non-

face small targets by jointly limiting the effective area (Equation (12)) and circumference (Equation (13)). Besides, according to the facial geometric characteristics of oval, it used the value interval (Equation (15)) of the circularity factor (Equation (14)) of connected targets to distinguish the face and non-face larger targets. Accordingly the non-face larger regions that was close in size but different in shape to the non-face regions can be removed.

$$S_k \in (S \times 5\% \quad S \times 90\% \quad) \tag{12}$$

$$F_K \in (10 \quad 22500) \tag{13}$$

$$C_k = F_k^2 / S_k \tag{14}$$

$$C_k \in (\ 5 \ \ 20\ ) \tag{15}$$

Where, S is total area of the whole image, K is serial number of the connected target, S_k , F_k, and C_k are the effective area, circumference, circularity of the first K connected target.

The steps of multiple-face detection are described as follows:

Step 1: Fast label the connected regions of the skin-segmented image (T_b), calculate effective area (S_k) and circumference (F_k) of the connected targets.

Step 2: Remove the noises or some non-face small regions by combined limiting the effective areas and the circumferences.

Step 3: Calculate circularity factors (C_k). By limiting the range of circularity factors, remove the non-face larger targets and acquire the real face targets.

By limiting the geometric features, the acquired multiple-face segmented image is shown in Figure 3(g). Contrasting Figure 3(f), it is easy to find that, the non-face skin regions (e.g. the palms, arms, and legs), the possible skin-similar regions, and the noises in the face candidates were removed.

5. Results and Discussion

5.1. Experimental Results and Analysis

The platform of experiments is: P4 2.10GHz CPU, 2G memory, WinXP, VC6.0. The proposed method was applied in the experiments on two multiple-face test sets. The built test set 1 contains 200 images, which consisted of 100 two-person, 50 three-person, and 50 4-or-more-person images. Table 1 summarizes the face extraction results based on test set 1, which contain 662 faces with variations. The Detection Rate (DR) is defined as the ratio of the number of correctly detected faces to the total number of faces in all images. The (FPR) is defined as the ratio of the number of detected false positives to the total number of faces. The False Positive Rate (FNR) is defined as the ratio of the number of false negatives to the total number of faces. The built test set 2 contains 300 images, which consisted of 150 images with abnormal exposure and 150 images with interfering backgrounds or fake objects. Table 2 lists the performance comparison of proposed method and other methods based on test set 2. Comparing with the other methods, there is no need to preprocess, train classifiers, and analyze lots of statistical samples for acquiring fixed parameters of model or interval threshold in proposed method. It acquired skin likelihood and initial clustering centers by the built YIC model, and acquired adaptive fuzzy clustering weights by the built YIQ model. From Table 2, the detection rate of proposed method is higher than that of other methods, but the false positive rate of proposed method is lower than that of other methods.

Table 1. Performance Comparison of 2-person, 3-person, and 4-or-more-person

	No. of Images	No. of Faces	No. of CD	No. of FP	No. of FN	DR	FPR	FNR
2-person	100	200	197	9	3	98.5	4.5	1.5
3-person	50	150	146	11	5	97.3	7.5	3.3
4-or-more-person	50	312	304	26	15	97.4	8.3	4.8
Total	200	662	647	46	23	97.7	6.9	3.5

Table 2. Performance Comparisons of Proposed Method and other Methods

Detection Methods	Test Set / Faces			
	Abnormal Exposure/457		Interfering Backgrounds/472	
	DR	FPR	DR	FPR
Detection using Gaussian Model [3]	84.6	14.5	85.5	15.8
Detection using Ellipse Model [2 5]	84.7	13.9	86.2	14.3
Detection using Adaboost [7 9]	85.6	15.6	85.7	16.2
Detection using Neural Network [8 9]	84.3	6.9	86.3	7.6
Detection using Template Matching [4]	94.3	7.3	95.8	8.1
Detection using Proposed Method	98.2	6.5	97.5	7.2

CD: Correct Detection, FP: False Positive, FN: False Negative,
DR(%): Detection Rate, FPR(%): False Positive Rate, FNR(%): False Negative Rate.

Figure 3. The Results of Skin Segmentation and Face Detection with Proposed Algorithm
(a) Multiple-face input images, (b) Skin-segmented images of (a) based on CbCr Gaussian model, (c) Skin-segmented images of (a) based on CbCr ellipse model, (d) Skin-likelihood images based on proposed YIC model, (e) Skin-probability images based on proposed YIQ model, (f) Skin-segmented images based on proposed model (YIC and YIQ dual skin model), (g) Face-detected images based on proposed method.

The experimental examples with different conditions (Low exposure, complicated backgrounds and glasses, complicated backgrounds and fake object, high exposure and fake object) are shown in Figure 3 and Figure 4. Figure 3 shows the results of skin segmentation and face detection with proposed algorithm. Figure 4 shows results of multiple-face extraction. In process of detection, the scaling strategy is used to image normalization for handling very large image, which is up to 4 million pixels. However, the memory consuming of detection was only 8-12M, and the average time consuming was 70~80ms (12.5~14fps). Through experiments, it is clear that, for poor-quality color face image with abnormal exposure and interfering backgrounds, the proposed algorithm had satisfactory speed, accuracy and adaptability of detection.

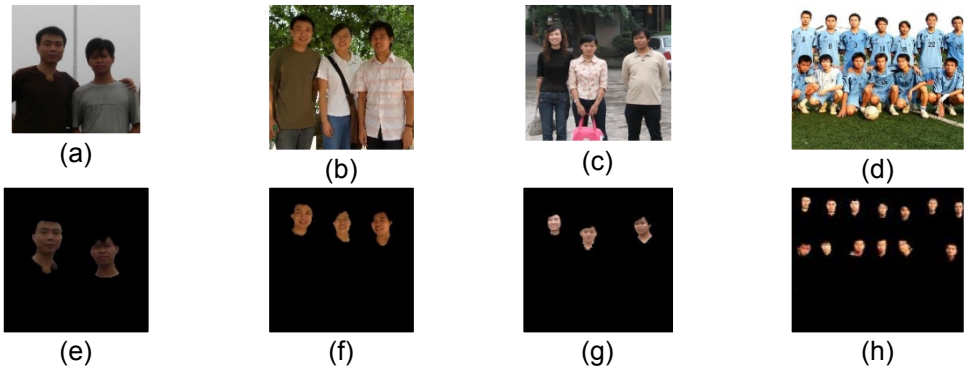

Figure 4. The Examples of Multiple-face Extraction
(a) Two-person image (with low exposure), (b) Three-person image (with complicated backgrounds and glasses), (c) Three-person image (with complicated backgrounds and fake object), (d) Three-person image (with high exposure and fake object), (e)Face-extracted image of (a), (f) Face-extracted image of (b), (g) Face-extracted image of (c), (h) Face-extracted image of (d).

5.2. Discussion of Proposed Algorithm

The main features of this algorithm are as follows:

1. There was no need to preprocess and train the classifier. By combining the luminance (Y), the differences of the chrominance (Cb, Cg, and Cr) and I component, this algorithm established the adaptive multiple-component YIC skin model. The calculated skin likelihood based on YIC model can reflect the clustering characteristics of skin color, and help to resistant to luminance variations and backgrounds interfering.

2. Using the distribution characteristic of normalized skin likelihood, the adaptive initial clustering centers of FCM was acquired by the automatic histogram analysis and searching. This decreased the invalid calculation and the clustering instability caused by the unsuitable initial clustering centers, which helped to improve the speed, accuracy and adaptability of fuzzy clustering segmentation.

3. Combining I, Q components and their expectations, this algorithm established the adaptive YIQ skin-probability model. The skin probability based on YIQ model was regarded as the dynamic clustering weights to reduce the invalid calculation of clustering and promote the clustering convergence as soon as possible. Using the initial clustering centers and the dynamic clustering weights, the improved computational formula of membership degree was proposed. The improved FCM clustering segmentation was benefit for improving the speed, accuracy and adaptability of segmentation.

4. Jointly using and limiting three factors (the effective area, circumference, and circularity) of connected targets in skin-segmented image, the non-face regions in face candidates were removed fast, which increased the correct detection rate.

6. Conclusion

This study provided an adaptive and fast detection algorithm of multiple-face targets. It established two adaptive skin models, based on which it acquired the skin-likelihood image for clustering, the adaptive initial clustering centers and fuzzy clustering weights. Then it adopted the improved FCM clustering to segment and to acquire the skin targets. Finally it distinguished the face targets by jointly limiting the areas, circumferences, and circularities of the connected targets. The experimental results show that, for the multiple-face images with interfering backgrounds, fake objects, and abnormal exposure, this algorithm has satisfactory speed, accuracy, and adaptability of face detection.

Acknowledgements

This work was supported in part by the Sichuan Provincial Department of Science and Technology Supporting Project (No. 2012GZ0020), the Natural Science Key Foundation of

Sichuan's Province Education Department (No. 11ZA041), the Key Project of Education Department of Sichuan Province (No. 13ZA0015), the Scientific Research Foundation of the Education Department of Sichuan Province of China (No. 13ZB0012).

References

[1] Abate AF, Nappi M, Riccio D, Sabatino G. 2D and 3D Face Recognition: A Survey. *Patt. Recog. Lett*. 2007; 28: 1885-1906.
[2] Zhang DZ, Wu BY, Sun JB, Liao QL. *A Face Detection Method based on Skin Color Model*. Proceedings of the 11th Joint Conference on Information Sciences. Shenzhen, China. 2008; pp: 1-5.
[3] Shih FY, Cheng SX, Chuang CF, Wang PSP. Extracting Faces and Facial Features from Color Images*. Int. J. Pattern Recognit. Artif. Intell*. 2008; 22: 515-534.
[4] Wang Z, Li S. Face Recognition using Skin Color Segmentation and Template Matching Algorithms. *Inf. Technol. J.* 2011; 10: 2308-2314.
[5] Hsu RL, Abdel-Mottaleb M, Jain AK. Face Detection in Color Images. *Trans. Pattern Anal. Mach. Intell.* 2002; 24: 696-706.
[6] Ruiz-del-Solar J, Quinteros J. Illumination Compensation and Normalization in Eigenspace-based Face Recognition: A Comparative Study of Different Pre-processing Approaches*. Pattern Recognit. Lett.* 2008; 29: 1966-1979.
[7] Yang M, Crenshaw J, Agustine B, Mareachen R, Wu Y. AdaBoost-based Face Detection for Embedded Systems. *Comput. Vision Image Understanding*. 2010; 114: 1116-1125.
[8] Yang J, Liu C, Zhang L. Color space normalization: Enhancing the Discriminating Power of Color Spaces for Face Recognition. *Pattern Recognit.* 2010; 43: 1454-1466.
[9] Wang Z, Li T. *A Face Detection System based Skin Color and Neural Network*. Proceedings of the International Conference on Computer Science and Software Engineering. Wuhan, China. 2008; pp: 961-964.
[10] Guo JM, Lin CC, Wu MF, Chang CH, Lee H. Complexity Reduced Face Detection using Probability-based Face Mask Prefiltering and Pixel-based Hierarchical-feature Adaboosting. *IEEE Signal Process Lett.* 2011; 18: 447-450.
[11] Chaves-Gonzalez JM, Vega-Rodriguez MA, Gomez-Pulido JA, Sanchez-perez JM. Detecting Skin in Face Recognition Systems: A Colour Spaces Study. *Digital Signal Processing.* 2010; 20: 806-823.
[12] C Lin, Qin X, Zhu GL, Wei JH, Lin C. Face Detection Algorithm Based on Multi-orientation Gabor Filters and Feature Fusion. *TELKOMNIKA Indonesian Journal of Electrical Engineering.* 2013; 11(10): 5986-5994.
[13] Wang YT, Li WB, Pang S, Kan JM. Segmentation Method of Lingwu Long Jujubes Based on L*a*b* Color Space. *TELKOMNIKA Indonesian Journal of Electrical Engineering*. 2013; 11(9): 5344~5351.